Research Article | Vol. 6, No. 11 | 1 Nov 2016 | OPTICAL MATERIALS EXPRESS 3670

Optical Materials EXPRESS

Optimization of the liquid crystal light valve for signal beam amplification

KONSTANTIN SHCHERBIN,[1,*] IGOR GVOZDOVSKYY,[1] AND DEAN R. EVANS[2]

[1]*Institute of Physics, National Academy of Sciences, Prospekt Nauki 46, 03680 Kiev, Ukraine*
[2]*Air Force Research Laboratory, Materials and Manufacturing Directorate, Wright-Patterson Air Force Base, OH 45433, USA*
**kshcherb@iop.kiev.ua*

Abstract: A liquid crystal light valve is an optically controlled spatial light modulator made as a cell with liquid crystal on a photoconductive substrate. Dynamic holograms recorded in such a hybrid device may give rise to the amplification of one of the recording beams at the expense of the other. In the present work, liquid crystal light valves with different thicknesses of the liquid crystal layer are studied at various conditions of the dynamic grating recording aiming to maximize the signal beam amplification in the infrared. A seventeen-fold gain is achieved in the improved cell for optimal recording conditions.

OCIS codes: (190.2055) Dynamic gratings; (230.6120) Spatial light modulators; (160.3710) Liquid crystals; (160.6000) Semiconductor materials; (260.3060) Infrared.

References and links

1. J. Grinberg, A. Jacobson, W. Bleha, L. Miller, L. Fraas, D. Boswell, and G. Myer, "A new real-time non-coherent to coherent light image converter – The hybrid field effect liquid crystal light valve," Opt. Eng. **14**(3), 217–225 (1975).
2. P. Aubourg, J. P. Huignard, M. Hareng, and R. A. Mullen, "Liquid crystal light valve using bulk monocrystalline $Bi_{12}SiO_{20}$ as the photoconductive material," Appl. Opt. **21**(20), 3706–3712 (1982).
3. D. R. Evans and G. Cook, "Nonlinear Optics: Research continues to advance photorefractive beam coupling," Laser Focus World **41**(12), 67–70 (2005).
4. D. R. Evans, G. Cook, V. Yu. Reshetnyak, C. M. Liebig, S. A. Basun, and P. P. Banerjee, "Inorganic–organic photorefractive hybrids," in *Springer Series in Materials Science vol. 240*, P. A. Blanche, ed. (Springer, 2016).
5. T. Sasaki, "Dynamic Amplification of Optical Signals by Photorefractive Ferroelectric Liquid Crystals," in *Ferroelectric Materials – Synthesis and Characterization*, A. Peláiz-Barranco, ed. (InTech, 2015).
6. W. Lee and S. L. Yeh, "Optical amplification in nematics doped with carbon nanotubes," Appl. Phys. Lett. **79**(27), 4488–4490 (2001).
7. I. C. Khoo, C. W. Chen, and T. J. Ho, "Observation of photorefractive effects in blue-phase liquid crystal containing fullerene-C_{60}," Opt. Lett. **41**(1), 123–126 (2016).
8. I. Gvozdovskyy, K. Shcherbin, D. R. Evans, and G. Cook, "Infrared sensitive liquid crystal photorefractive hybrid cell with semiconductor substrates," Appl. Phys. B **104**(4), 883–886 (2011).
9. A. Peigné, U. Bortolozzo, S. Residori, S. Molin, P. Nouchi, D. Dolfi, and J. P. Huignard, "Adaptive holographic interferometer at 1.55 μm based on optically addressed spatial light modulator," Opt. Lett. **40**(23), 5482–5485 (2015).
10. K. Shcherbin, I. Gvozdovskyy, and D. R. Evans, "Infrared sensitive liquid crystal light valve with semiconductor substrate," Appl. Opt. **55**(5), 1076–1081 (2016).
11. V. Marinova, C. H. Chi, Z. F. Tong, R. C. Liu, N. Berberova, S. H. Lin, Y. H. Lin, E. Stoykova, and K. Y. Hsu, "Liquid crystal light valve operating at near infrared spectral range," Opt. Quantum Electron. **48**(4), 270 (2016).
12. U. Bortolozzo, S. Residori, and J. P. Huignard, "Beam coupling in photorefractive liquid crystal light valves," J. Phys. D Appl. Phys. **41**(22), 224007 (2008).
13. W. R. Roach, "Resolution of electrooptic light valves," IEEE Trans. Electron Dev. **ED-21**(8), 453–459 (1974).
14. V. F. Nazvanov and D. I. Kovalenko, "Resolution of optically addressed liquid-crystal spatial light modulators," Tech. Phys. Lett. **24**(7), 520–522 (1998).

1. Introduction

It is known that dynamic holograms may be recorded in different hybrid liquid crystal cells. In such devices a driving force is created inside a photosensitive substrate. This driving force affects liquid crystals (LC) and creates in it a spatial modulation of the refractive index. Due to the huge birefringence of LC the amplitude of the index modulation may be very large.

#276048 http://dx.doi.org/10.1364/OME.6.003670
Journal © 2016 Received 19 Sep 2016; revised 14 Oct 2016; accepted 15 Oct 2016; published 27 Oct 2016

Optical Materials EXPRESS

Therefore the diffraction efficiency of the grating created in a thin LC layer may be sufficiently high for many applications including amplification of a weak signal beam.

Two main types of hybrids may be distinguished. These are liquid crystal light valves (LCLV) and photorefractive–LC hybrids. To the best of our knowledge, the LCLV working in the reflection geometry was the first reported hybrid cell. Devices of this type are actively studied as Spatial Light Modulators (SLM) and have been since 1970s [1]. The use of a transparent photoconductive substrate made from bulk crystalline $Bi_{12}SiO_{20}$ allowed operation of LCLV in the transmission geometry [2]. The driving force in LCLV is a light-induced spatial modulation of the voltage formed in a photoconductive substrate. In the photorefractive–LC hybrids [3,4] the space-charge field affects the spatial alignment of the LC molecules. As a result the refractive index in the LC also becomes spatially modulated.

Dynamic grating recording was also reported for LC blends where driving force is created in photosensitive dopants. These are ferroelectric LC [5], nematic LC with carbon nanotubes [6], blue-phase LC containing fullerene-C_{60} [7], etc. The large exponential gain factor $\Gamma > 10^3$ cm^{-1} was reported [5,6] for such mixtures. However the amplification factor is important for many tasks. It may be relatively small in a thin LC layer even with a large gain factor.

The devices sensitive in the infrared spectral range are especially interesting as they are well-matched for available telecommunication components. The recording of dynamic gratings in this spectral range was demonstrated recently for both types of hybrids [8–11].

In the present work, we are focusing on LCLV because such devices ensure larger amplification of a weak signal light wave [10,12]. A fourfold gain was reported for grating recording in GaAs-based LCLV at wavelength $\lambda = 1.06$ μm [10]; our aim is to increase this gain. For this purpose beam coupling is studied in the cells with different thickness of the LC layer for applied voltage with various amplitudes and frequencies. Spatial resolutions of the devices are compared. The thicknesses of the LC layer and the conditions of the grating recording are optimized for maximizing amplification of the weak signal wave.

2. LCLV principle and experimental set-up

The general design of the LCLV operating in the transmission geometry is shown in Fig. 1(a). The input window is made out of a photoconductive material (PhC). The output window is a glass plate. Two transparent indium tin oxide (ITO) electrodes are deposited on the substrate and glass window in such a way that the voltage is applied across the substrate and LC. When the photoconductive substrate is illuminated by the interference pattern created by two intersecting light waves, as it is shown in Fig. 1(a), the resistance of the substrate becomes spatially modulated. As a result, the voltage across LC also becomes spatially modulated. LC molecules are reoriented and a refractive index grating is created in the LC layer.

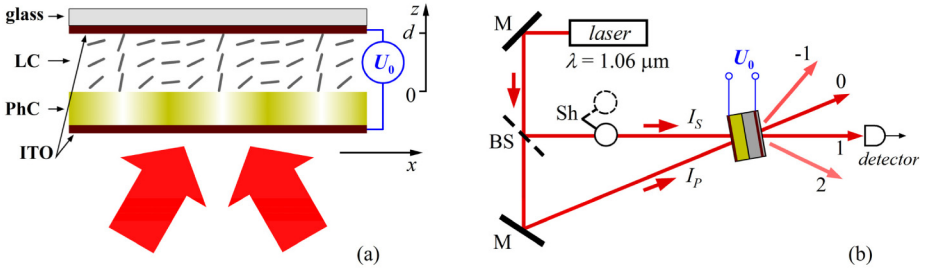

Fig. 1. (a) – Schematic sketch of the LCLV, and (b) – experimental set-up; see text for details.

The photoconductive substrate in our cell is an optically finished 8 × 15 mm^2 GaAs plate with thickness $h = 1.1$ mm. Nominally undoped semi-insulating GaAs single-crystal exhibits a dark resistivity of the order of 5×10^8 Ohm × cm. The cell is filled with BL006 (Merck) LC. Mechanically rubbed polyimide alignment layer deposited on the inside face of the semiconductor substrate and on the glass face coated by ITO ensures planar orientation of the

Optical Materials EXPRESS

LC. The LC layer thickness d is set by spherical glass spacers. The cells with d = 5, 10, 16 μm are studied. For this purpose the LCLV was reassembled with different spacers using the same GaAs substrate. Sinusoidal ac voltage is applied to the ITO electrodes.

It is important that the conductivity grating in the substrate is local and dynamic. The index grating in LC is pinned to the conductivity grating; therefore, the index grating is a fixed thin local grating with respect to the recording interference fringes. Such a grating may give rise to the amplification of the weak recording beam due to diffraction of light from the strong pump beam in the direction of the weak signal [12]. We study this amplification.

The experimental set-up is shown schematically in Fig. 1(b). A single-mode single-frequency diode-pumped Nd^{3+}:YAG laser emitting at λ = 1.06 μm is used as a light source. The output laser radiation polarized in the plane of incidence is expanded and divided by a variable beam splitter BS into two beams I_P and I_S with a typical intensity ratio $\beta = I_P(z=0)/I_S(z=0) \approx 80$. Both beams have a Gaussian intensity distribution with about 20 mm full-width at half maximum on the cell input face. The diaphragm with a diameter of 5 mm placed on the input face of the cell cuts the central part of the recording beams ensuring spatial homogeneity of the light intensity within ± 4%. In this way the formation of a nonlinear lens in the LCLV is minimized. The total light intensity I = 30 mW/cm^2.

Two beams I_P and I_S are crossed in the GaAs window and initiate the index grating formation in the LC. High diffraction orders appearing behind the cell show that the grating is thin and self-diffraction in the Raman-Nath regime is observed. To separate the transmitted signal beam from the pump its intensity is measured behind the 0.5 mm diameter diaphragm placed at the focal plane of a lens with 25 cm focal length. Electrical impedances of the illuminated and unilluminated photoconductive substrate are different. To keep the electrical properties of the LCLV nearly constant the strong pump beam is continuously sent through the cell. The shutter Sh allows blocking/unblocking the signal beam. The temporal envelopes of the intensity of the transmitted signal are recorded in the cells with different thickness of the LC layer under different experimental conditions. The steady state gain of the signal beam $G = I_S / I_{S0}$ is evaluated from the temporal envelopes, where I_S and I_{S0} are intensities of the signal beam behind the cell with and without the pump beam, respectively. Intensity I_{S0} without the pump is measured at time t = 0, when the signal beam is unblocked but the dynamic hologram is not recorded yet.

3. Experimental results and discussion

The LCLV cells have relatively low spatial resolution [2] because the voltage modulation created in the substrate is blurred strongly in the LC along z-direction. Theory predicts that the cells with thinner LC layers exhibit better spatial resolution [2,13]. On the other hand it is evident that gratings in a thicker LC layer ensures larger diffraction efficiency. To find a compromise between spatial resolution good enough for reliable grating recording and large amplification of the signal, we study the gain as a function of spatial frequency N of the recorded grating. Experimental data are shown by symbols in Fig. 2 for the cells assembled with the same GaAs substrate but with the LC layers of different thicknesses. The cell with thinner LC (d = 5 μm) demonstrates the better spatial resolution with flat region at low spatial frequency. The largest gain is reached in the LCLV with the thickest LC layer (d = 16 μm) at spatial frequency N = 1 lp/mm (line pairs per mm), which is the smallest possible value in our experiment for reliable separation of the signal beam from the pump behind the cell.

The weak beam is amplified in the LCLV because of light diffraction from the strong pump in the direction of the signal. For a large beam ratio $\beta >> 1$ the diffraction efficiency of a thin grating created in the LC is small $\eta << 1$. The last fact is confirmed in the experiment: only –1 and + 2 orders of diffraction with respect to the pump beam (see Fig. 1(b)) are observed behind the LCLV. The diffraction efficiency may be simplified in this case

Optical Materials EXPRESS

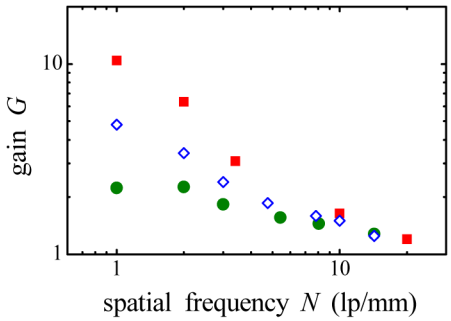

Fig. 2. Gain as a function of spatial frequency measured in LCLV with thicknesses of the LC layer: green circles – d = 5 μm, blue diamonds – d = 10 μm, and red squares – d = 16 μm.

$$\eta = \left(\pi \Delta n\, d/\lambda\right)^2, \tag{1}$$

where Δn is the amplitude of refractive index modulation. Then, taking into account the diffraction from the pump, the intensity and the gain of the signal beam may be found

$$I_S(d) = I_S(0) + \eta I_P(0) = I_S(0) + \left(\pi \Delta n\, d/\lambda\right)^2 I_P(0), \tag{2}$$

$$G = I_S(d)/I_S(0) = 1 + \eta\beta = 1 + \beta\left(\pi \Delta n\, d/\lambda\right)^2. \tag{3}$$

The proportionality expression for the refractive index modulation follows from Eq. (3)

$$\Delta n \propto \sqrt{G-1}. \tag{4}$$

This refractive index modulation may be used for characterization of the recorded grating. On the other hand spatial voltage modulation in the cell is also small at large beam ratios and the refractive index change in the LC is proportional to the voltage modulation. Its dependence on spatial frequency was considered in the early works on different light valves [2,10]

$$\frac{\Delta U(N)}{\Delta U(N \to 0)} = \frac{1}{\pi N} \frac{\varepsilon_{PhC}/h + \varepsilon_z/d}{\varepsilon_{PhC} \coth\left(\pi N h\right) + \sqrt{\varepsilon_x \varepsilon_z} \coth\left(\pi N d \sqrt{\varepsilon_x/\varepsilon_z}\right)} \tag{5}$$

where ε_{PhC} is the dielectric permittivity of the isotropic substrate, while ε_x and ε_z are the dielectric permittivities of the LC along corresponding axis; $\varepsilon_x = \varepsilon_{\|}$ and $\varepsilon_z = \varepsilon_{\perp}$ for planar alignment of LC with no applied voltage, where $\varepsilon_{\|}$ and $\varepsilon_{\perp}$ are the handbook values of the components along and perpendicular to the director, respectively.

Thus, an obvious way to compare spatial resolution measured in the experiment with existing theory is to set a correspondence between Eq. (4) and Eq. (5):

$$\sqrt{G-1} \propto \frac{1}{\pi N} \frac{\varepsilon_{PhC}/h + \varepsilon_z/d}{\varepsilon_{PhC} \coth\left(\pi N h\right) + \sqrt{\varepsilon_x \varepsilon_z} \coth\left(\pi N d \sqrt{\varepsilon_x/\varepsilon_z}\right)}. \tag{6}$$

The symbols in Fig. 3(a) represent experimental data presented in Fig. 2 replotted as a function $[G(N) - 1]^{1/2}$ normalized to the value for $N \to 0$. The lines of the corresponding colors in Fig. 3(b) represent calculations according Eq. (5) with $\varepsilon_{PhC} = 12.9$ for GaAs and with $\varepsilon_x = \varepsilon_{\|} = 20$, $\varepsilon_z = \varepsilon_{\perp} = 4.7$ for BL006.

It is clear from Fig. 3(a) that the spatial bandwidth is reduced when the LC layer becomes thicker. Theoretical lines in Fig. 3(b) qualitatively describe well the experimental data showing the same tendency. However the measured spatial bandwidth is smaller than it is predicted by Eq. (5). One of the known reasons for such discrepancy is diffusive spreading and drift of the photo-excited carriers in the photoconductor [14]. Another factor is the light

Optical Materials EXPRESS

scattered in the substrate and the light reflected back inside it from different components of the LCLV; this light decreases the contrast. The decrease is more pronounced at higher spatial frequencies and therefore the parasitic light narrows the spatial bandwidth of the LCLV. Some additional factors that may be important for quantitative disagreement are: a pump depletion for large gain, uncertainties of the thickness of LC and its permittivity components, presence of ions in the LC, and large-scale space charge formation in the substrate.

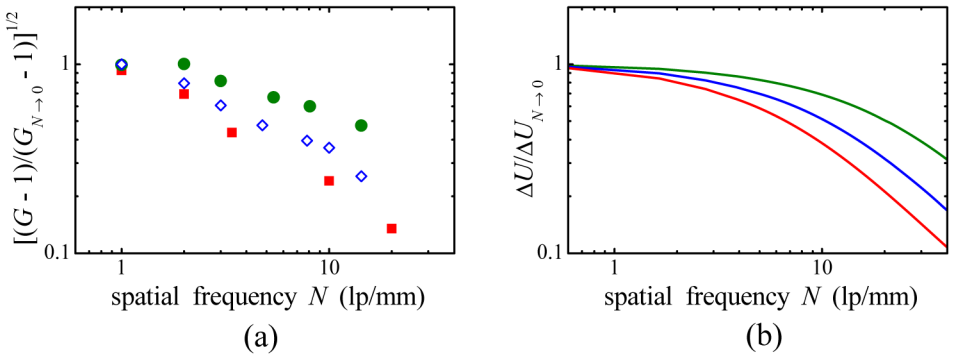

Fig. 3. Spatial frequency dependence of the (a) – measured gain replotted as $[G(N) - 1]^{1/2}$ and (b) – light-induced spatial modulation of the voltage across LC calculated according Eq. (5). The LC layer thicknesses are: green – d = 5 μm, blue – d = 10 μm, and red – d = 16 μm. Applied voltage with peak amplitude U_0 = 10 V and optimal frequency f_{opt} = 200 kHz; beam ratio β = 80; light intensity I = 30 mW/cm^2.

An equivalent electrical circuit of the LCLV includes several *RC*-circuits, which correspond to different layers of the cell [1,2]. That is why a maximum voltage across LC layer is reached at a resonant frequency. Naturally, a similar resonance is observed for the gain. It is presented in Fig. 4(a) where the gain of the signal beam is shown as a function of frequency of the applied voltage with peak amplitude U_0 = 10 V measured in the cell with d = 16 μm at a spatial frequency N = 1 lp/mm. The largest gain G ≈11 is measured at the resonance frequency f_{opt} = 200 kHz.

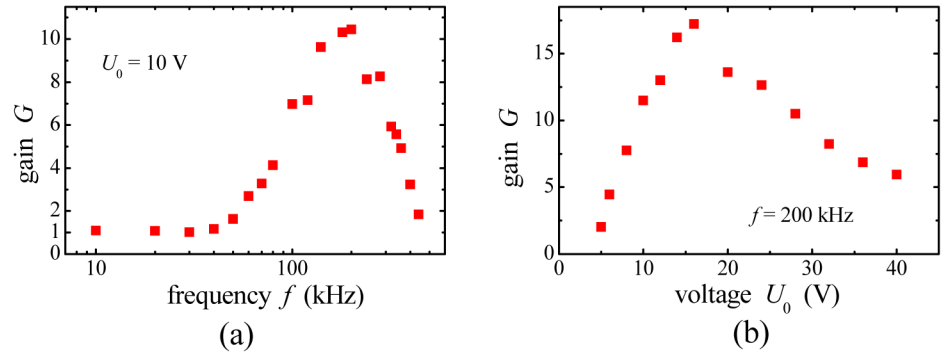

Fig. 4. Gain of the signal beam measured as a function of: (a) – frequency of the applied voltage with peak amplitude U_0 = 10 V and (b) – peak amplitude of the applied voltage at the optimal frequency f_{opt} = 200 kHz. Spatial frequency N = 1 lp/mm; beam ratio β = 80; light intensity I = 30 mW/cm^2.

A tilt of LC molecules on the same small angle results in a largest refractive index change when the director is aligned at 45° to the planar orientation. On the other hand a larger driving force is necessary to achieve the same tilt of the LC molecules when the pretilt is large. Therefore the voltage ensuring the largest possible gain corresponds to the tilt somewhere below 45°. To find this optimal voltage we measure the gain as a function of applied voltage

Optical Materials EXPRESS

at optimal frequency f_{opt} = 200 kHz. Experimental dependence presented in Fig. 4(b) shows that the largest gain G = 17.2 is achieved with voltage U_0 = 16 V. To the best of our knowledge, this gain is the largest gain ever reported for LCLV. The temporal envelope of the signal corresponding to this gain is shown in Fig. 5 by the red line. Initially the intensity increases quadratically because amplification is determined by the diffraction efficiency, which is proportional to the square of the refractive index change. Then the signal intensity increases and reaches its steady state value with a characteristic time $\tau \approx 0.2$ s. The blue line in Fig. 5 shows for comparison the data describing the gain previously reported for other GaAs-based LCLV [10] with d = 10 μm operating at Λ = 440 μm with applied voltage U_0 = 2.6 V. Obviously, considerable increase of the amplification is achieved in the present work.

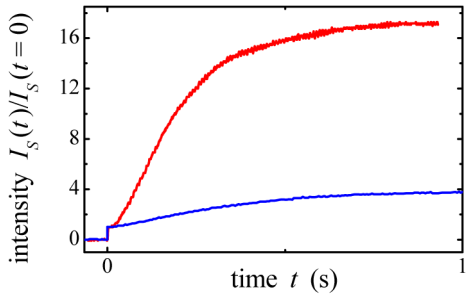

Fig. 5. Temporal envelope of the signal beam intensity measured in the cell with d = 16 μm at Λ = 1000 μm with optimal amplitude and frequency of the applied voltage (red line). Blue line shows for comparison the signal beam amplification achieved in another LCLV with d = 10 μm at Λ = 440 μm.

4. Conclusions

In the present work optimal conditions are found for large signal beam amplification using dynamic gratings recorded in the LCLV. The signal beam gain G = 17 is achieved at λ = 1.06 μm for small contrast recording in GaAs-based LCLV with a 16-μm-thick LC layer. This gain is 4 times larger than G = 4 reported previously for similar LCLV cell [10] operating in the infrared. To the best of our knowledge, this is the largest gain ever reported for any LCLV.

Good spatial resolution is crucially important for image processing with SLM. The LCLV with thinner LC layer has better spatial bandwidth with flat region at low spatial frequency. The LCLV can operate as SLM in this case processing images without nonlinear distortions. On contrary, the interaction length and coupling constant product define the strength of interaction. That is why naturally the larger gain is reached in a thicker LC. In this case a low spatial resolution requires operation at small spatial frequencies. Our results confirm that LCLV with a thick LC layer cannot be used as SLM for processing of high resolution images. However, it can be effectively used for signal beam amplification. If a particular task allows operation at low spatial frequency, a large amplification of the signal beam can be achieved.

On the other hand, the spatial bandwidth of the LCLV is defined by a thinner layer, either a LC or photoconductive substrate, as the denominator in Eq. (6) predicts. For a large gain, a considerable spatial voltage modulation is required. Hypothetically it could be achieved even in a thin substrate with low dark conductivity but remarkable photoconductivity. If such a material could be found, a large gain could be achieved in LCLV with much better spatial resolution, which would be defined by a thin photoconductive substrate with $h << d$.

Funding

European Office of Aerospace Research and Development (EOARD) (11-8006); Science and Technology Center in Ukraine (STCU) (P585).